計算機에 의한 回轉型電磁增幅機의 動特性 및 減磁作用 影響에 관한 해석적 연구

논 문
22~1~1

Analytical Study of the Machine Dynamics of the Amplidyne Under the Demagnetization Effect

장 세 훈*
(Se Hoon Chang)

Abstract

This paper is for the supplementary studies of the theoretical treaties on the machine dynamics of the amplidyne generator under the influencies of the armature reaction. The author has already shown the time-domain expression of the dynamic relations of the machine with balanced control winding, under this operating condition.

In this paper, analytical and experimental studies of a test machine are intended to supplement the theories derived in the previous work, entitled "On the dynamics and the demagnetization effect of the amplidyne generator with auxiliary feedback compensating winding". FACOM 230 digital computer is incorporated for processing of a series of experimental data. The machine dynamics are then numerically analyzed with the aid of the computer. The virtual machine responses to stepwise inputs are compared with the computer output to confirm the influence of the armature reaction effect on to the machine dynamics.

1. Introduction

The state models of the amplidyne under the influence of the armature reaction effect have already formulated in the three-dimensional state space with the set of state variables, i_f, i_q, and i_o. The necessary assumptions for the derivation of the dynamic models were;

a) the machine constants are assumed to be time-invariant.

b) the mechanical structure of the machine is assumed to be symmetrical in their physical constructions.

c) the demagnetization flux is directly proportional to load current.

d) the residual flux and magnetic recoil effect due to the slots and tooth are neglected.

e) the direct-axis component of the magnetic flux due to the quadrature winding current is assumed to be negligible.

f) the control field currents and the feedback current are assumed not to contribute any significant effects on to the quadrature axis flux component.

For the conveniencies, the state models of the machine dynamics derived in the previous work are tabulated below;

*정회원 : 한양대학교 공과대학 교수

$$\begin{pmatrix} \frac{di_f}{dt} \\ \frac{di_q}{dt} \\ \frac{di_o}{dt} \end{pmatrix} = \begin{pmatrix} -R_f/(L_f+M_f) & O & [(M_{do}-M_{cf})d/dt]/(L_f+M_f) \\ K_{fq}/L_q & -R_q/L_q & [K_{dq}+(M_{dq}-M_{cq})d/dt]/L_q \\ (-M_{fc}d/dt)/(L_o-M_{dc}) & K_{qd}/(L_o-M_{dc}) & -(R_L+R_{dc})/(L_o-M_{dc}) \end{pmatrix} \begin{pmatrix} i_f \\ i_q \\ i_o \end{pmatrix}$$

$$+ \begin{pmatrix} 1/(L_f+M_f)[M_{of}d/dt]/(L_f+M_f) \\ O \qquad -K_f/L_q \\ O \qquad [M_{co}d/dt]/(L_o-M_{dc}) \end{pmatrix} \begin{pmatrix} e_1 \\ i_o \end{pmatrix} \quad (1\text{-}1)$$

with the output relation;

$$e_o = Z_L i_o \quad (1\text{-}2)$$

For the properly compensated machine from the demagnetization effect, both of the control and the quadrature winding circuit are completely decoupled from the influence due to the load current, i_o and hence $M_{dq}=M_{dq}$, $M_{cq}=M_{dq}$, and $K_{dq}=O$ should. be saticified. Then, this state model is further reduced into;

$$\begin{pmatrix} \frac{di_f}{dt} \\ \frac{di_q}{dt} \\ \frac{di_o}{dt} \end{pmatrix} = \begin{pmatrix} -R_f/(L_f+M_f) & O & O \\ K_{fq}/L_q & -R_q/L_q & O \\ [-M_{fc}d/dt]/L_L & K_{qd}/L_L & -(R_L+R_{dc})/L_L \end{pmatrix} \begin{pmatrix} i_f \\ i_q \\ i_o \end{pmatrix}$$

$$+ \begin{pmatrix} 1/(L_f+M_f)[M_{of}d/dt]/(L_f+M_f) \\ O \qquad -K_f/L_q \\ O \qquad [M_{co}d/dt]/L_L \end{pmatrix} \begin{pmatrix} e_1 \\ i_o \end{pmatrix} \quad (1\text{—}3)$$

and, for the output equation;

$$e_o = Z_L i_o \quad (1\text{—}4)$$

The state model for the unloaded machine can be formulated as shown below, by setting certain terms to zero in equation (1-1) and equation(1-2).

$$\begin{pmatrix} \frac{di_f}{dt} \\ \frac{di_q}{dt} \end{pmatrix} = \begin{pmatrix} -R_f/(L_f+M_f) & O \\ K_{fq}/L_q & -R_q/L_q \end{pmatrix} \begin{pmatrix} i_f \\ i_q \end{pmatrix}$$

$$+ \begin{pmatrix} 1/(L_f+M_f)[-M_{of}d/dt]/(L_f+M_f) \\ O \qquad -K_f/L_q \end{pmatrix} \begin{pmatrix} e_1 \\ i_o \end{pmatrix} \quad (1\text{—}5)$$

and the output equation becomes;

$$e_o = -M_{fc}\frac{di_f}{dt} + K_{qd}i_q + M_{co}\frac{di_o}{dt} \quad (1\text{—}6)$$

2. Quantitative Experiment on the Machine Dynamics

(1) General description of experimental set-ups

Figure 1 shows the connection details of the experimental set-ups for this test. The amplidyne generator under the investigation has the

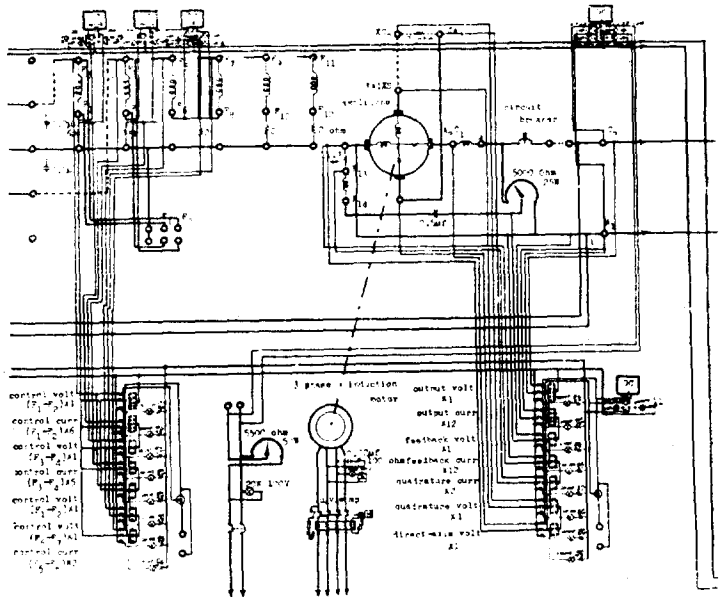

그림 1. 실험장치의 결선도

Fig. 1. Connection diagram of the set-ups.

following specifications and ratings supplied from the manufacturer of the machine;

type AM, frame 79A, 125 volts, 1500 watts, 1800 rpm direct coupled to and on the same base with induction motor, type K, frame 77, 220 volts, 3-phase, 60 cycles, 1800 rpm.

The 3-phase induction motor embeded with the generator section of the machine is fed from the 3-phase AC power source through a differential ground-fault circuit breaker to ensure the safety from the electrical hazards. All of the winding terminals of the machine is brought to the front and is displayed onto the control panel so that they may provide cooperative terminal connections. Point-contact relays are incorporated to facilitate the measurements of the machine characteristics, with proper metering schemes for monitoring the machine operation. The balanced control winding of the amplidyne generator is driven from the difference servo amplifiers constructed. To provide a load onto the generator, a DC geared motor is arranged and is armature-controlled by connecting to the output terminals of the machine.

(2) Determination of machine parameters

To determine the resistive part of the windings and the transfer constants of the machine, the V-I characteristics of each individual winding are measured (DC test) and the data are numerically approximated by the use of the linear least squares criterion, with the highest probability of the best representation of the experimental data, as in the followings. The data are obtained by forcing n equi-intervaled values of current expressed in ma to flow through the winding and the voltage drop across the winding terminals is recorded in volt.

The current values and the voltage readings in order are denoted by x and y, respectively, in the computer program, and they are read in to the computer by the READ statement.

Using the least squares criterion,

$$\frac{\partial \sum_{i=1}^{n} e_i^2}{\partial a_0}=0, \text{ and } \frac{\partial \sum_{i=1}^{n} e_i^2}{\partial a_1}=0 \qquad (2-1)$$

In this expression, a_1 is the slope of the V-I characteristic curve and a_0 is the intersection of this linear approximated curve with the voltage axis in the V-I plane. The two unknowns, a_0 and a_1, may be subsequently determined, noting that,

$$e_i=y_i-(a_0+a_1x_1) \qquad (2-2)$$

The least squares criterion is now reduced into the following discreted-data form, that is;

$$\left.\begin{aligned}&\frac{\partial \sum_{i=1}^{n} (y_i-(a_0+a_1x_i))^2}{\partial a_0}=0\\ &\text{and}\\ &\frac{\partial \sum_{i=1}^{n} (y_i-(a_0+a_1x_i))^2}{\partial a_1}=0\end{aligned}\right\} \qquad (2-3)$$

Simplifying these equations, the recursion expression is reduced to;

$$\left.\begin{aligned}&na_0+a_1\sum_{i=1}^{n}x_i-\sum_{i=1}^{n}y_i=0\\ &\text{and}\\ &a_0\sum_{i=1}^{n}x_i+a_1\sum_{i=1}^{n}x^2{}_1-\sum_{i=1}^{n}x_iy_i=0\end{aligned}\right\} \qquad (2-4)$$

which may be solved for the values of a_0 and a_1. For the computer programming purposes, these may be written as;

N*AO+ONE*SMX=SMY

and

AO*SMX+AONE*SQX=SMXY

From which,

AO=(SMX*SMXY−SQX*SMY)/(SMX*SMX-N*SQX)

and

AONE=(SMY-N*AO/SMX)

The ohmic value of the winding resistance is found from the slope of this linear least squares line multiplied by 10^3 and the transfer constants of the machine in volt/milliamps are obtained from the intersection of the voltage axis of it's V-I characteristic curve, AO. The computer program with the experimental data is supplemented in Appendix.

For the determination of the inductances of the windings, a series of measurements for the v-i characteristics is carried out (AC test) and the data are approximated, at this time, by their arithmatic mean values, and the self and mutual inductances of the windings are evaluated by substituting the resistance of the corresponding winding. The computer program and the exper-

imental data are also shown in Appendix.

The final output from FACOM 230-13 is tabulated below in Table 1.

표 1. 측정된 시험기의 기계정수

Table 1. Machine parameters obtained.

SYMBOL	VALUES IN OHM OR IN H	AVERAGE VALUES
RFI	923.15878 ohms	923.15878 ohms
RF2	925.76022 ohms	925.76022 ohms
RA	59.58538 ohms	59.58538 ohms
RC	0.71358 ohms	0.71358 ohms
RQ	3.80 ohms (iq=0.6A) 1.1818 ohms (iq=5.5A)	2.07455 ohms
RD'+KDD	4.70 ohms (io=0.5A) 5.80 ohms (io=1.0A)	5.26975 ohms
KFQ	480 V/A (il=10 ma) 520 V/A (il=20 ma)	
KDQ	24.0 V/A (id=100 ma)	
KF	11.8 V/A (ia=100 ma)	
KQD	34.16 V/A (iq=0.6 A) 24.54 V/A (iq=5.5 A)	
LFI	49.0120 H (il=10 ma) 52.9834 H (il=20 ma)	50.9977 H
LF2	49.0110 H (il=10 ma) 58.2424 H (il=20 ma)	53.6267 H
LA	2.1420 H (ia=20 ma) 2.3820 H (ia=40 ma)	2.2620 H
LC	0.1530 H (ic=0.5 A) 0.3000 H (ic=1.0 A)	0.2260 H
LQ	0.1530 H (iq=0.5 A) 0.1390 H (iq=1.0 A)	0.1460 H
LD'	0.1980 H (id=0.5 A) 0.2000 H (id=1.0 A)	0.1990 H
M21	46.9510 H (i2=10 ma) 54.3160 H (i2=20 ma)	50.6335 H
M12	16.9510 H (il=10 ma) 54.3780 H (il=20 ma)	50.6645 H
MAF1	17.612 H (ia=20 ma) 20.690 H (ia=40 ma)	19.151 H
MAF2	17.612 H (ia=20 ma) 20.556 H (ia=40 ma)	19.084 H
MCF1	2.334 H (ic=10 ma) 3.394 H (ic=20 ma)	2.864 H
MCF2	2.450 H (ic=10 ma) 3.2078 H (ic=20 ma)	2.8289 H
MFC	0.281 H (il=5 ma) 0.150 H (il=10 ma)	0.4088 H
MCA	0.071 H (ia=20 ma) 0.041 H(ia=40 ma)	0.0647 H
MCQ	0.169 H (ic=200 ma) 0.217 H (ic=500 ma)	0.1703 H or 0.4558 H
MDQ	0.375 H (id=200 ma) 0.344 H (id=300 ma)	0.3730 H
(MCQ(minus)MDQ)	0.091 H (ic=id=1 A) 0.084 H (ic=id=2 A)	0.0828 H
MDE	6.046 H (id=100 ma)	6.2712 H

	6.550 H (id=200 ma)	
(MCF-(minus)MDE)	0.124 H (ic=id=1 A) 0.114 H (ic=id=2 A)	0.1248 H
MCF	6.3960 H	6.3960 H
MDC	0.1703 H	0.1703 H

3. Numerical Anaysis of the Machine Dynamics

Equation (1—1) in section 1 is the general expression of the dynamic relation of the machine. By setting certain terms to zero, in this expression, the machine dynamics can be obtained for different load and compensating conditions from the demagnetization effect. The output relation is also available from the result of eguation (1—2).

Almost any of the techniques which are used to solve a single-order differential equation may be used to solve a set of simultaneous first-order differential equations, i.e., a matrix first-order differential equation. In order to extend the improved Euler method to the solution of a set of simultaneous first-order differential equations as defined by equation (1—1), equation (1—1) and equation (1—2) are rearranged in the following general concised-form, thus;

$$\dot{Y}(t)=G(Y,t) \qquad (3—1)$$

where G is a matrix function of t and Y.

Let;

$$\begin{aligned} &G_1=G(t_i, Y_i)\\ &G_2=G(t_i+\Delta t, Y_i+G_1\cdot\Delta t)\\ &\cdots\cdots\cdots\cdots\cdots\\ &\cdots\cdots\cdots\cdots\cdots\\ &Y_{i+1}=Y_i+(G_1+G_2)\frac{\Delta t}{2} \end{aligned} \qquad (3—2)$$

where Y_i is a k-element column matrix defining the value of the state variables $Y_{(t)}^{(k)}(k=1,2,3)$ at some value t_i of time, and Y_{i+1} is the column matrix defining the new values of the three state variables $Y_{(t)}^{(k)}$ at t_{i+1} sec., as found by the application of the Quinn's numerical technique. Similarly, G_1 is a column matrix with k elements $G_1^{(k)}$ determined by evaluating the matrix function G at the values of it's arguments (t_i, Y_i), and G_2 is a column matrix at the values of it's arguments $(t_i+\Delta t,\ Y_i+G_1\Delta t)$. The new values of the states as specified by the column matrix Y_{i+1} are used as the starting point for a new determination of additional values of the elements of $Y_{(t)}$, and the process is continued iteratively to the desired final

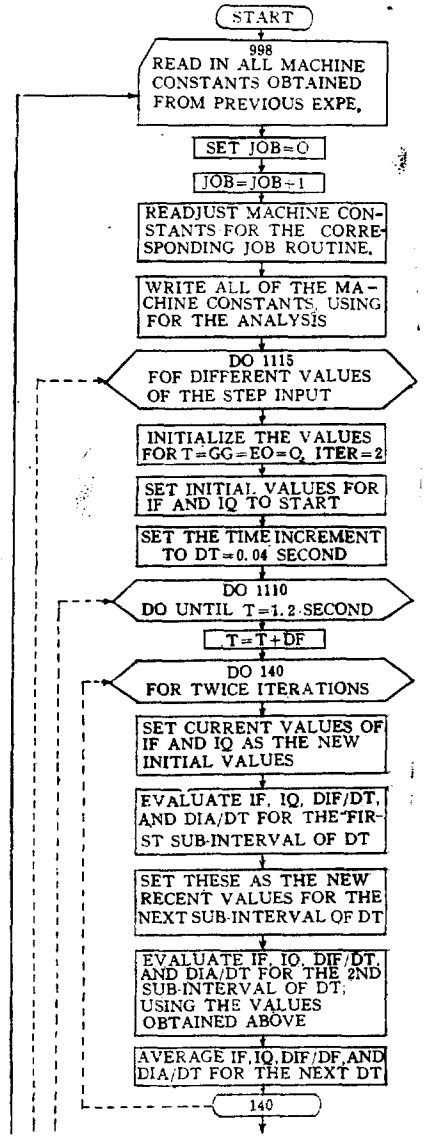

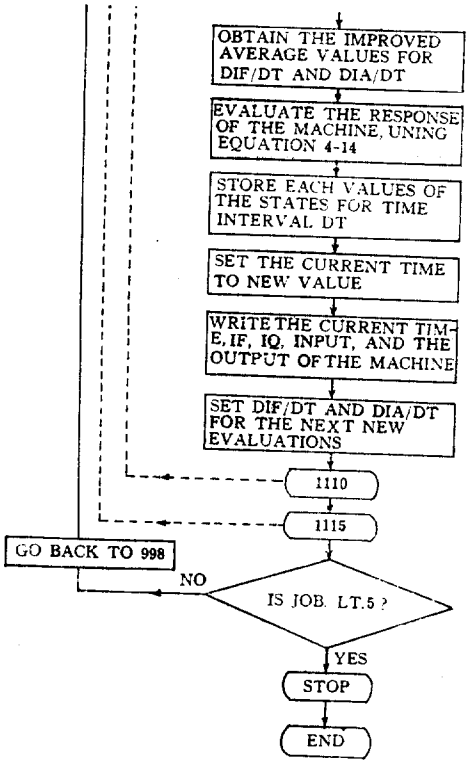

그림 2. JOB routines에 대한 flow-chart.
Fig. 2. Simplified flow-chart for jobs.

value of t.

Figure 2 shows the outlined flow-chart for the computer program.

JOB 1, JOB 2, JOB 3 JOB 4, and JOB 5 in the flow-chart, are for the program for each of the following cases;

JOB 1; the machine is not compensated from the demagnetization effects, at all. The machine is loaded by 100-ohm external resistor.

JOB 2; the machine is compensated from the demagnetization effects, but the comepensation is not proper. The machine is also loaded by 100-ohm external resistor.

JOB 3; the machine is properly compensated from the demagnetization effects,. The machine is loaded by 100-ohm external resistor.

JOB 4; the machine is not compensated from the demagnetization effects. The machine is not loaded.

JOB 5; the machine is compensated from the demagnetization effects and operates under no-load condition.

In each case, the machine constants are read in or evaluated, first and let the computer set the parameters adequately so as to meet the loading and the compensating conditions imposed upon each of the cases as specified previously. For each of the JOB routines, the three state variables, i_f, i_q, i_o and the output response are evaluated numerically, for four different values of the step-wise input to the machine; 4.62 volts, 9.23 volts, 13.85 volts and 18.46 volts in magnitude. The virtual responses of the machine are observed by the use of Model 150A/AR HEWLETT PACKARD dual trace Oscilloscope. The output from FACOM 230—10 computer is plotted in figure 3, imposing the virtual response of the machine on the same sheet, for the comparisons between the virtual and analytical results. (note: because of the paper limitation, two of them are shown, here).

It may be noticeable that when the machine parameters are treated to be constants through out the whole range of the machine operation, profound discrepancies from the virtual response are measured as shown in the figure. These linearized versions may fail to represent the virtual machine dynamics in good accuracy.

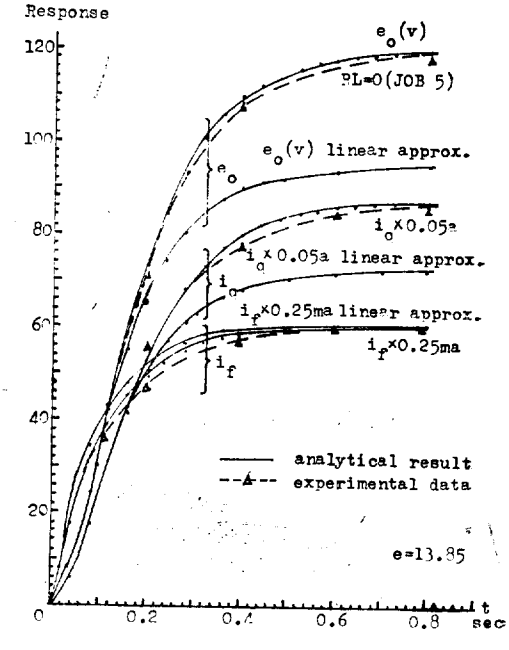

(a)

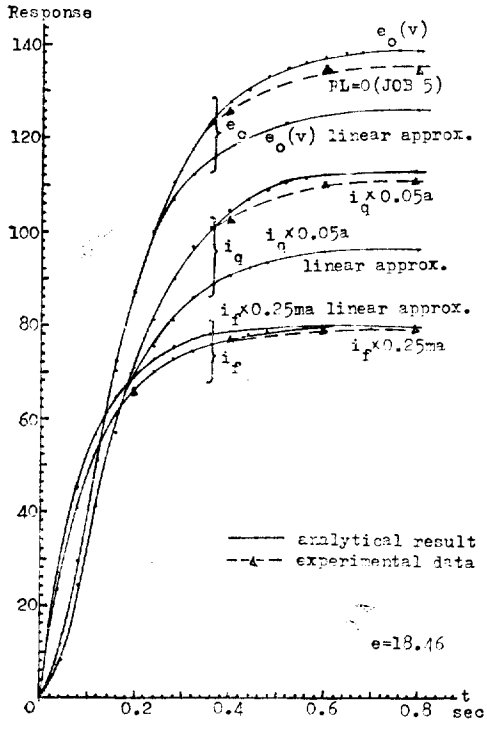

(b)

그림 3. 계단상 압력에 대한 시험기의 응답
(감자작용이 보상되고, 무부하된 조건하)
Fig. 3. Machine responses to step-wise inputs (compensated, and under no-load condition)

4. On the Effect of Non-Linearities

Up to this point, the machine parameters; the effective resistances of the windings, the self and the mutual inductances, and the transfer constants of the test machine are treated to be constant and their values are assumed to remain on a certain constant values over the full range of the machine operation. In this section, the effects of the non-linearity shall be taken into account for the final development.

On determining the effective resistance of the windings, the experimental data supplemented in Appendix have shown quite good agreements with the linear approximation of the resistances, except for the resistances in the quadrature-axis and the direct-axis winding circuits. Figure 4 shows the virtual variation of these effective resistances; RQ and RD'+KDD.

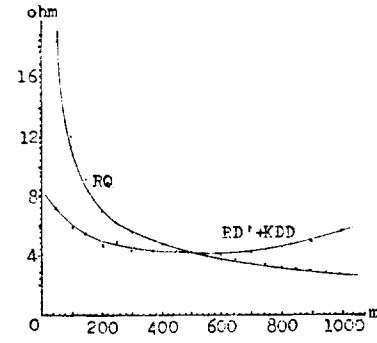

그림 4. RQ 및 RD'+KDD의 실측치
Fig. 4 Virtual variation of RQ and RD'+KDD.

To interpolate the effective resistance values of these circuits, the following interpolation scheme is intended.

Let $f(i_1)$, $f(i_2)$, and $f(i_3)$ be the discrete-data values obtained from the v-i characteristics of a circuit, for equi-distant current values forced through the circuit, i_1, i_2, and i_3, and $f(i)$ is assumed to be well approximated by the follo wing second order polynomial,

$$f(i)=a_0+a_1i^1+a_2i^2$$

Since the polynomial is required to pass through the data points measured by the v-i characteristic curve, it should satisfy the following equalities;

$$a_0+a_1i_1+a_2i_1^2=f(i_1)$$
$$a_0+a_1i_2+a_2i_2^2=f(i_2)$$
$$a_0+a_1i_3+a_2i_3^2=f(i_3)$$

The three unknowns; a_0, a_1, and a_2 now can be evaluated by the Crout method.

The influence of the variation in contact-resistance of the carbon brushes involved in these circuits should be the primary factor of this non-linearity, in company with the magnetic saturation and the variation of the magnetic permidity.

Since the self and the mutual inductances of the windings are also associated with the non-linear magnetic circuit of the machine, it is well expected that these shall be under the influence of this non-linear effect. The virtual experiments have shown in figure 5. The variation of the magnetic permidity and the magnetic saturation of the core are understood to be

responsible for these non-linear relations depicted in the figure.

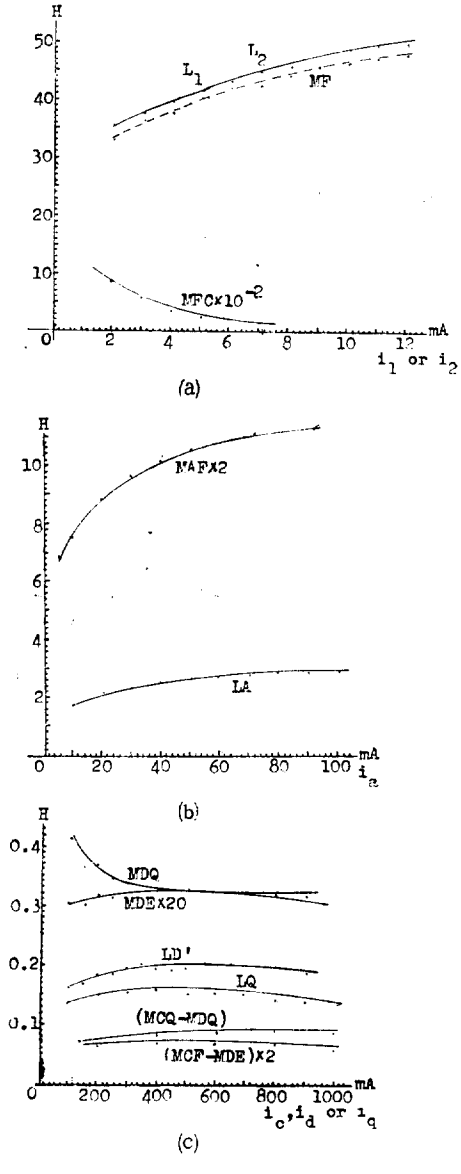

그림 5. 시험기의 각권선의 인덕턴스의 실측값
Fig. 5. Virtual variation of the inductances of the test machine.

Figure 6 shows the variation of the transfer constants over a certain region of the machine operation. In order to represent the machine parameters with more good accuracy, taking into account these influences by the non-linearity the experimental data are approximated with second-order polynomials by the use of the Crout method. The computer program is attached in Appendix and the output results are tabulated in table 2, below.

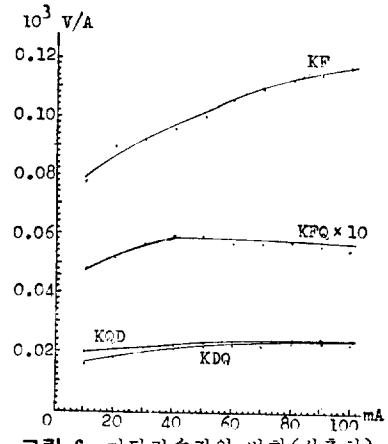

그림 6. 전달정수값의 변화(실측치)
Fig. 6. Virtual variation of the transfer constants.

The general procedure of this approximation may be explained by the same interpolating scheme discussed previously.

표 2. 시험기의 기계정수들의 略算式
Table 2. Approximated polynomials of machine parameters

machine constants	approximated polynomials
RQ	$5.63818-0.00331i+0.00000i^2$
RD′+KDD	$6.20000-0.00840i+0.00001i^2$
KFQ	$453.30005+2.00503i+0.06650i^2$
KDQ	$13.68889+0.24533i-0.00142i^2$
KF	$71.44444+0.67667i-0.00211i^2$
KQD	$24.75443+0.00556i-0.00000i^2$
M12	$31.443+1.90675i-0.0381i^2$
M21	$30.549+2.03075i-0.04212i^2$
MAF1/2	$5.26404+0.23561i-0.00246i^2$
MAF2/2	$5.29571+0.24517i-0.00271i^2$
MAC	$0.23549+0.01087i-0.0000i^2$
MCA	$0.14562+0.00486i$
MF1C	$1.128+0.23187i-0.00828i^2$
MF2C	$1.146+0.2405i-0.009120i^2$
MCF1/2	$0.32979+0.07456i-0.00031i^2$
MCF2/2	$0.3465+0.10787i-0.002250i^2$
L1	$30.853+2.49212i-0.06928i^2$
L2	$34.444+1.61912i-0.02146i^2$
LA	$1.835+0.01662i-0.00006i^2$
LC	$0.07133+0.00102i-0.00000i^2$
LQ	$0.12666+0.00016i-0.00000i^2$
LD′	$0.14633+0.00015i-0.00000i^2$

where i is in ma.

Using these non-linear functions approximated as the machine parameters, the machine dynamics are programed on the computer, in the similar fashion as that of the previous section. The major difference in this time is in the expression of equation (3—1). G, at this time, is a non-linear matrix function of t and Y. It is interesting to note that the variation of the indutances has shown very little effects on the final analysis, but the variational influences of RQ and RD'+KDD terms and the transfer constants are very critical in the analysis of the final results.

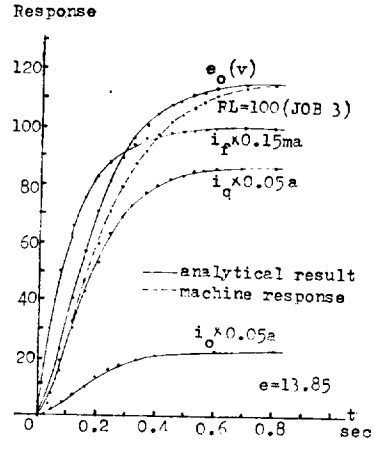

(a)

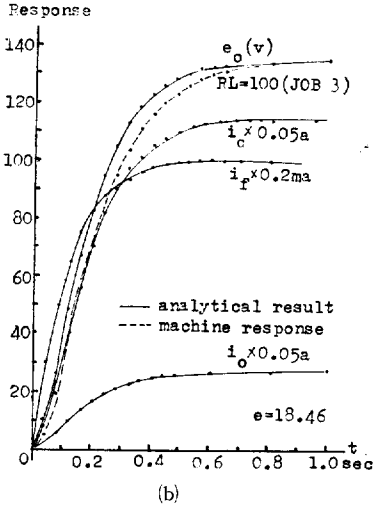

(b)

그림 7. 계단상 입력에 대한 기계의 응답(감자작용이 적절히 보상되고, 100ohm의 외부저항으로 부하된 경우)

Fig. 7 Response to step inputs (properly compensated, loaded with 100-ohm resistor)

Figure 7 is the response of the machine to step-wise inputs when the machine is loaded by 100-ohm external resistor and is properly compensated from the demagnetization effect. The analytical results under these circumstances reveal quite accurate agreements with the virtual response of the test machine.

5. Machine Dynamics Under the Demagnetization Effect

To investigate the machine dynamics under the demagnetization effect, the state transitions for the three cases; the properly compensated case, the improperly compensated case, and the case under the demagnetization effect, are compared in figure 8. The heavy lines in the figure show the responses of the properly compensated machine from the demagnetization. This may be considered as an idealized condition from the demagnetization effect. They are obtained with the use of equation (1—3), by substituting the machine parameters of the test machine. The light lines are for the responses of the same machine under the demagnetization effect. They depict rather slow transient responses than the earlier case. The actual machine responses of the test machine are shown by the dashed lines in the figure.

At the steady state, the transitions of the state variables of the machine can be derived from equation (1—1), equation (1—2), equation (1—3), and equation (1—6) and the results are;

$$\left.\begin{aligned} &-R_f i_f+e_1=0\\ &K_{fq}i_f-R_q i_q+K_{dq}i_o-K_f i_o=0\\ &K_{qd}i_q-(R_L+R_d+K_{dd})i_o=0\\ &\text{and}\\ &e_o=K_{fq}R_L[R_q(R_L+R_d+K_{dd})\\ &\quad-K_{dq}K_{qd}]e_1/K_{qd}R_f\\ &\quad-K_f R_L[R_q(R_L+R_d+K_{dd})\\ &\quad-K_{dq}K_{qd}]i_o/K_{qd} \end{aligned}\right\} \quad (5—1)$$

for the uncompensated and for the improperly compensated machine.

And

$$\left.\begin{aligned} &R_f i_f+e_1=0\\ &K_{fq}i_f-R_q i_q-K_f i_o=0\\ &K_{qd}i_q-(R_L+R_d+K_{dd}-K_{cq})i_o=0 \end{aligned}\right\}$$

and

$$\left.\begin{aligned} e_s = {} & K_{fq}R_L\,[R_q(R_L+R_d+K_{dd} \\ & -K_{cd})]\,e_1/K_{qd}R_f \\ & -K_fR_L\,[R_q(R_L+R_d+K_{dd} \\ & -K_{cq})]i_s/K_{qd} \end{aligned}\right\} \quad (5\text{—}2)$$

for the properly compensated machine.

About one second is required for the test machine to reach to the steady state as shown in the figure. It is also shown that the steady state of the machine dynamics are dimished to lower values due to the demagnetization effect.

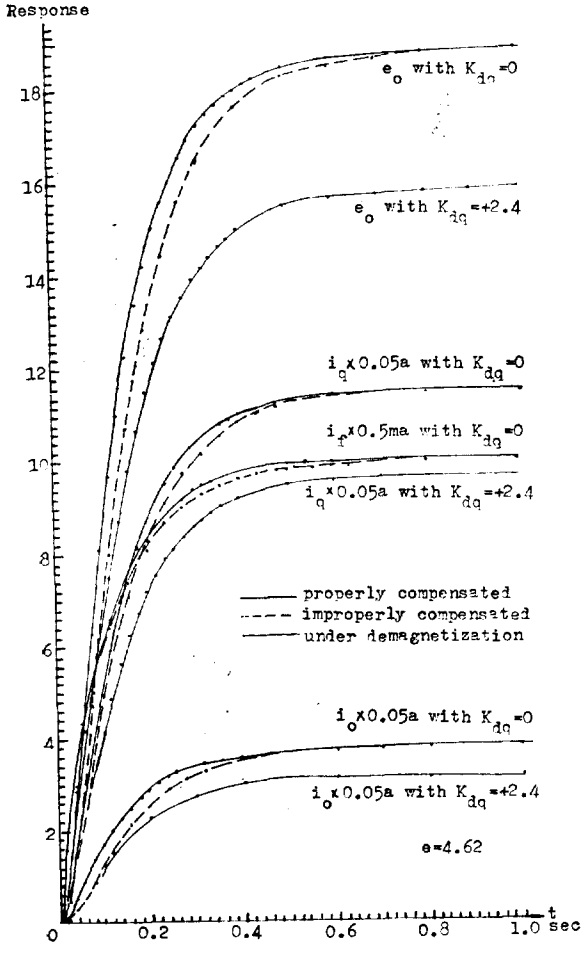

(a)

6. Conclusions and Discussions

Even under the linearized condition of the state model, the coefficient matrix of the machine dynamics is time variant. When the non-

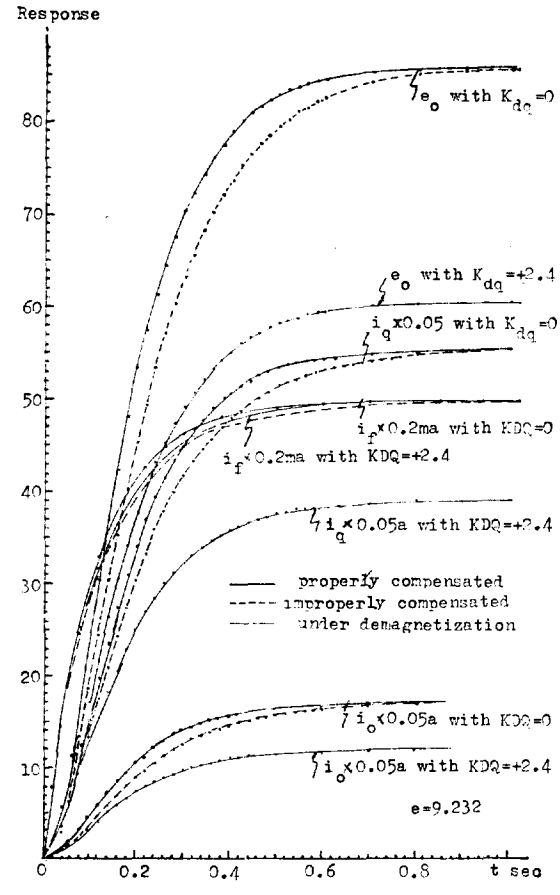

(b)

그림 8. 계단상 입력에 대한 시험기의 응답
100-ohm의 외부저항으로 부하된 경우

Fig. 8. Response to step inputs for the test machine, loaded with 100-ohm resistor.

linearities are taken into account in the analysis, the machine parameters are the non-linear function of the other state variables and certain elements in the coefficient matrix turn out to be non-linear and time-variant. The following may be concluded from the analytical results;

1) As well expected, the involution of the magnetic circuits and the brushes results the machine parameters to be non-linear funtions and time-variant. Hence, the machine dynamics can not be treated in a linearized fashion when a certain degree of accuracy is desired in the analysis for whole range of the machine operation.

2) The non-linearities due the variation in the inductances are notieable, but these affct very little onto the machine dynamics.
3) The resistances of the quadrature-axis and the direct-axis circuits, and the transfer constants reveal quite profound dependences on the non-linear effect. When the non-linear-variations are taken into account in the analysis, the results are in good agreement with the virtual response of the machine.
4) Under the influence of the demagnetization effects, the machine responses to step inputs are delayed, in time, tolerably in the order of 10 to 50 milliseconds for the test machine. The over-compensation from the demagnetization effect displays rather shorter rising-time, but with less relative stability of the machine operation.
5) At the steadt state, the machine dynamics are diminished to lower values by virtue of the demagnetization effect, as shown in equation (5—1) and equation (5—2).

References

1. M.L. James, G.M. Smith, J.C. Wolford, "Applied Numerical Methods for Digital Computation with Fortran, International Textbook Co., Pennsylvania, pp.313-451, 1968.
2. S.D. Conte, "Elementary Numerical Analysis", McGraw-Hill, New York, pp71-100, 1965.
3. S.H. Chang, "Study of the Non-linear Characteristics of Two- Phase Servomotor", Research News, N.C. State Univ., Ralcigh, N.C., 1962.
4. 張世勳, "PM型 制御用 Servo電動機의 Recoil動作에 관한 硏究" 대한전기학회지 제21권 제4호, 1972년 7월.
5. 自動制御理論, 韓萬春, 張世勳共著, 敎育院, 1971년 3월.
6. A. Dikarev, "Stability of the Amplidyne with Divided Magnetic System", Elektrotekhnika, Vol. 36, No.7, pp 19-21, 1965.
7. S.H. Chang, "On Performance Characteristics of Two-Phase Servomotors with and Without Feedback, M.S. Thesis, N.C. State Univ., Raleigh, N.C. 1962.
8. 自制制御論, 高橋安人編, 共立出版, pp.282—304, 1955.
9. 日本富士通, Facom 230—15 Fortan 文法編, Cat. No. SP—061—3—1.
10. 장세훈, "狀態變數에 의한 回轉型電磁增幅機의 動特性解析및 減磁作用効果에 관한 硏究" 大韓電氣學會誌 第21卷 第6號 pp. 9-16, 1972.